MMT-DY measurements with SPD.
Status and Plans.

SPD meeting 26.10.2017

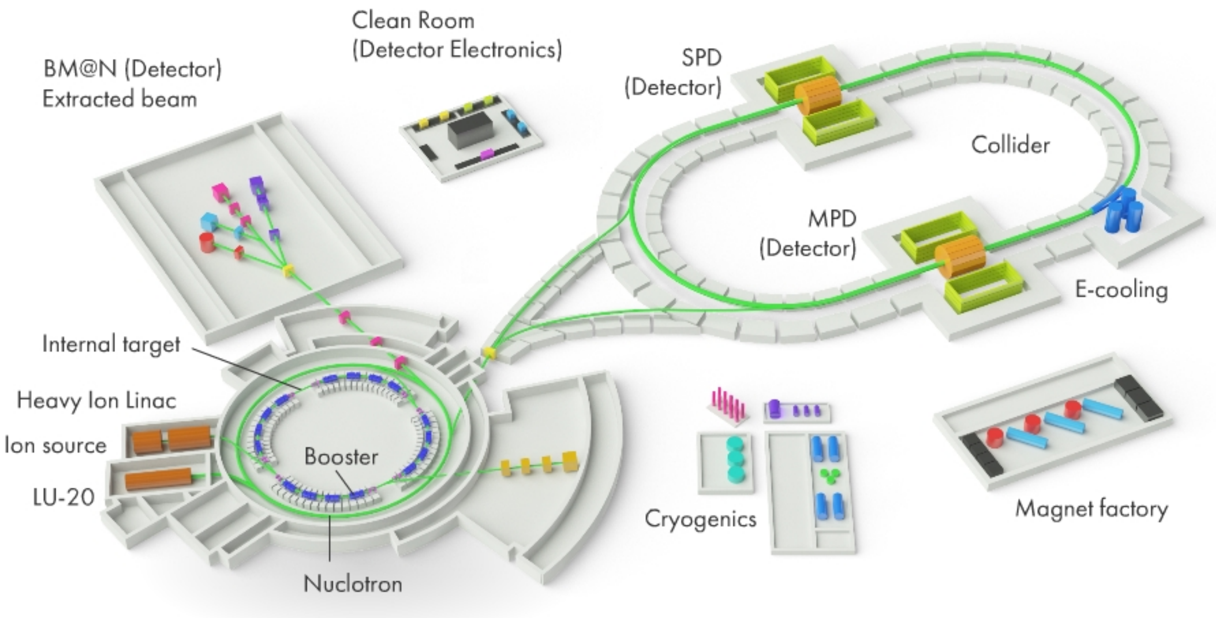

Nec sine te, nec tecum vivere possum. (Ovid)*

Introduction.

Now the quark-parton structure of nucleons and respectively the quark-parton model of nucleons are becoming more and more complicated. In Quantum Chromo Dynamics (QCD), PDFs depend not only on x, but also on Q^2, four-momentum transfer (see below). Partons can have an internal momentum, k, with possible transverse component, k_T . A number of PDFs depends on the order of the QCD approximations. Measurements of the collinear (integrated over k_T) and Transverse Momentum Dependent (TMD) PDFs, the most of which are not well measured or not discovered yet. (SPD LoI: e-Print:arXiv:1408.3959).

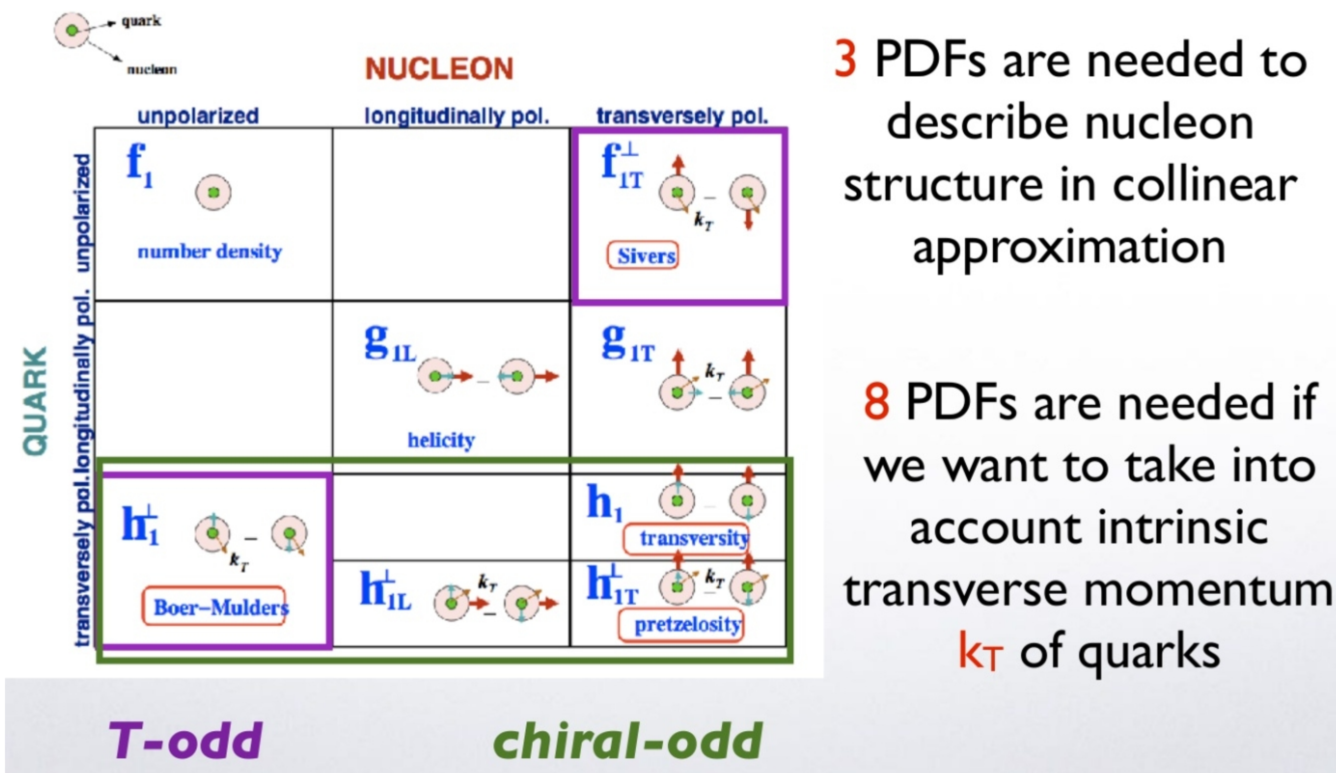

Physics motivations.

Nucleon spin structure studies using the MMT-DY reactions. The PDFs studies via asymmetry of the MMT-DY pairs.

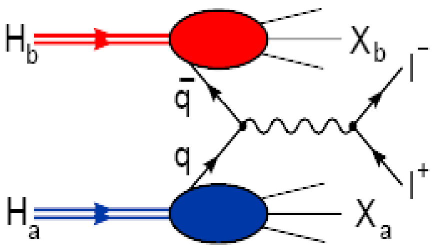

(a)

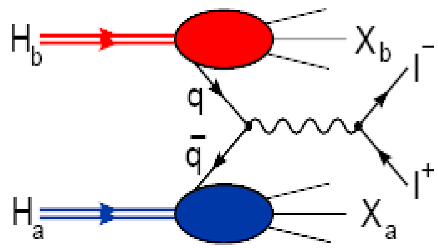

(b)

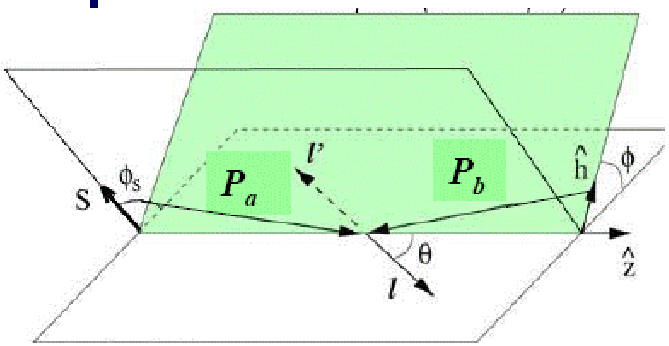

$$\frac{d\sigma}{dx_a dx_b d^2q_T d\Omega} = \frac{\alpha^2}{4Q^2}\times$$

$$\Big\{\Big((1+\cos^2\theta)F^1_{UU} + \sin^2\theta\cos 2\phi F^{\cos 2\phi}_{UU}\Big) + S_{aL}\sin^2\theta \sin 2\phi F^{\sin 2\phi}_{LU} + S_{bL}\sin^2\theta\sin 2\phi F^{\sin 2\phi}_{UL}$$

$$+\left|\vec{S}_{aT}\right|\Big[\sin(\phi-\phi_{S_a})\big(1+\cos^2\theta\big)F^{\sin(\phi-\phi_{S_a})}_{TU} + \sin^2\theta\Big(\sin(3\phi-\phi_{S_a})F^{\sin(3\phi-\phi_{S_a})}_{TU} + \sin(\phi+\phi_{S_a})F^{\sin(\phi+\phi_{S_a})}_{TU}\Big)\Big]$$

$$+\left|\vec{S}_{bT}\right|\Big[\sin(\phi-\phi_{S_b})\big(1+\cos^2\theta\big)F^{\sin(\phi-\phi_{S_b})}_{UT} + \sin^2\theta\Big(\sin(3\phi-\phi_{S_b})F^{\sin(3\phi-\phi_{S_b})}_{UT} + \sin(\phi+\phi_{S_b})F^{\sin(\phi+\phi_{S_b})}_{UT}\Big)\Big]$$

$$+S_{aL}S_{bL}\Big[\big(1+\cos^2\theta\big)F^1_{LL} + \sin^2\theta\cos 2\phi F^{\cos 2\phi}_{LL}\Big] \qquad (2.1.2)$$

$$+S_{aL}\left|\vec{S}_{bT}\right|\Big[\cos(\phi-\phi_{S_b})\big(1+\cos^2\theta\big)F^{\cos(\phi-\phi_{S_b})}_{LT} + \sin^2\theta\Big(\cos(3\phi-\phi_{S_b})F^{\cos(3\phi-\phi_{S_b})}_{LT} + \cos(\phi+\phi_{S_b})F^{\cos(\phi+\phi_{S_b})}_{LT}\Big)\Big]$$

$$+\left|\vec{S}_{aT}\right|S_{bL}\Big[\cos(\phi-\phi_{S_a})\big(1+\cos^2\theta\big)F^{\cos(\phi-\phi_{S_a})}_{TL} + \sin^2\theta\Big(\cos(3\phi-\phi_{S_a})F^{\cos(3\phi-\phi_{S_a})}_{TL} + \cos(\phi+\phi_{S_a})F^{\cos(\phi+\phi_{S_a})}_{TL}\Big)\Big]$$

$$+\left|\vec{S}_{aT}\right|\left|\vec{S}_{bT}\right|\Big[\big(1+\cos^2\theta\big)\Big(\cos(2\phi-\phi_{S_a}-\phi_{S_b})F^{\cos(2\phi-\phi_{S_a}-\phi_{S_b})}_{TT} + \cos(\phi_{S_b}-\phi_{S_a})F^{\cos(\phi_{S_b}-\phi_{S_a})}_{TT}\Big)\Big]$$

$$+\left|\vec{S}_{aT}\right|\left|\vec{S}_{bT}\right|\Big[\sin^2\theta\Big(\cos(\phi_{S_a}+\phi_{S_b})F^{\cos(\phi_{S_a}+\phi_{S_b})}_{TT} + \cos(4\phi-\phi_{S_a}-\phi_{S_b})F^{\cos(4\phi-\phi_{S_a}-\phi_{S_b})}_{TT}\Big)\Big]$$

$$+\left|\vec{S}_{aT}\right|\left|\vec{S}_{bT}\right|\Big[\sin^2\theta\Big(\cos(2\phi-\phi_{S_a}+\phi_{S_b})F^{\cos(2\phi-\phi_{S_a}+\phi_{S_b})}_{TT} + \cos(2\phi+\phi_{S_a}-\phi_{S_b})F^{\cos(2\phi+\phi_{S_a}-\phi_{S_b})}_{TT}\Big)\Big]\Big\}$$

where F^i_{jk} are the Structure Functions (SFs) connected to the corresponding PDFs. The SFs depend on four variables $P_a \cdot q$, $P_b \cdot q$, $\mathbf{q_T}$ and q^2 or on $\mathbf{q_T}$, q^2 and the Bjorken variables of colliding hadrons, x_a, x_b,

$$x_a = \frac{q^2}{2P_a \cdot q} = \sqrt{\frac{q^2}{s}}e^{y},\; x_b = \frac{q^2}{2P_b \cdot q} = \sqrt{\frac{q^2}{s}}e^{-y},$$ y is the CM rapidity and

The cross section cannot be measured directly because there is no single beam containing particles with the U, L and T polarization. To measure SFs entering this equation one can use the following procedure: first, to integrate cross section over the azimuthal angle *Φs*, second, following the SIDIS practice, to measure azimuthal asymmetries of the DY pair's production cross sections. The integration over the azimuthal angle *Φ* gives:

$$\sigma_{int} \equiv \frac{d\sigma}{dx_a dx_b d^2q_T d\cos\theta} = \frac{\pi\alpha^2}{2q^2}\times\big(1+\cos^2\theta\big)\Big[F^1_{UU} + S_{aL}S_{bL}F^1_{LL}$$

$$+\left|\vec{S}_{aT}\right|\left|\vec{S}_{bT}\right|\Big(\cos(\phi_{S_b}-\phi_{S_a})F^{\cos(\phi_{S_b}-\phi_{S_a})}_{TT} + D\cos(\phi_{S_a}+\phi_{S_b})F^{\cos(\phi_{S_a}+\phi_{S_b})}_{TT}\Big)\Big]$$

Physics motivations.

Nucleon spin structure studies using the MMT-DY reactions. The PDFs studies via asymmetry of the MMT-DY pair.

$$A_{UU} \equiv \frac{\sigma^{00}}{\sigma^{00}_{int}} = \frac{1}{2\pi}(1 + D\cos 2\phi\, A_{UU}^{\cos 2\phi})$$

$$A_{LU} \equiv \frac{\sigma^{\rightarrow 0} - \sigma^{\leftarrow 0}}{\sigma^{\rightarrow 0}_{int} + \sigma^{\leftarrow 0}_{int}} = \frac{|S_{aL}|}{2\pi} D\sin 2\phi\, A_{LU}^{\sin 2\phi}$$

$$A_{UL} \equiv \frac{\sigma^{0\rightarrow} - \sigma^{0\leftarrow}}{\sigma^{0\rightarrow}_{int} + \sigma^{0\leftarrow}_{int}} = \frac{|S_{bL}|}{2\pi} D\sin 2\phi\, A_{UL}^{\sin 2\phi}$$

$$A_{TU} \equiv \frac{\sigma^{\uparrow 0} - \sigma^{\downarrow 0}}{\sigma^{\uparrow 0}_{int} + \sigma^{\downarrow 0}_{int}} = \frac{|\vec{S}_{aT}|}{2\pi}\left[A_{TU}^{\sin(\phi-\phi_{S_a})} \sin(\phi - \phi_{S_a}) + D\left(A_{TU}^{\sin(3\phi-\phi_{S_a})} \sin(3\phi - \phi_{S_a}) + A_{TU}^{\sin(\phi+\phi_{S_a})} \sin(\phi + \phi_{S_a}) \right)\right]$$

$$A_{UT} \equiv \frac{\sigma^{0\uparrow} - \sigma^{0\downarrow}}{\sigma^{0\uparrow}_{int} + \sigma^{0\downarrow}_{int}} = \frac{|\vec{S}_{bT}|}{2\pi}\left[A_{UT}^{\sin(\phi-\phi_{S_b})} \sin(\phi - \phi_{S_b}) + D\left(A_{UT}^{\sin(3\phi-\phi_{S_b})} \sin(3\phi - \phi_{S_b}) + A_{UT}^{\sin(\phi+\phi_{S_b})} \sin(\phi + \phi_{S_b}) \right)\right]$$

$$A_{LL} \equiv \frac{\sigma^{\rightarrow\rightarrow} + \sigma^{\leftarrow\leftarrow} - \sigma^{\rightarrow\leftarrow} - \sigma^{\leftarrow\rightarrow}}{\sigma^{\rightarrow\rightarrow}_{int} + \sigma^{\leftarrow\leftarrow}_{int} + \sigma^{\rightarrow\leftarrow}_{int} + \sigma^{\leftarrow\rightarrow}_{int}} = \frac{|S_{aL} S_{bL}|}{2\pi}\left(A_{LL}^{1} + D A_{LL}^{\cos 2\phi} \cos 2\phi \right)$$

$$A_{TL} \equiv \frac{\sigma^{\uparrow\rightarrow} + \sigma^{\downarrow\leftarrow} - \sigma^{\downarrow\rightarrow} - \sigma^{\uparrow\leftarrow}}{\sigma^{\uparrow\rightarrow}_{int} + \sigma^{\downarrow\leftarrow}_{int} + \sigma^{\downarrow\rightarrow}_{int} + \sigma^{\uparrow\leftarrow}_{int}} = \frac{|\vec{S}_{aT}|\, S_{bL}}{2\pi}\left[A_{TL}^{\cos(\phi-\phi_{S_a})} \cos(\phi - \phi_{S_a}) + D\begin{pmatrix} A_{TL}^{\cos(3\phi-\phi_{S_a})} \cos(3\phi - \phi_{S_a}) \\ + A_{TL}^{\cos(\phi+\phi_{S_a})} \cos(\phi + \phi_{S_a}) \end{pmatrix}\right]$$

$$A_{LT} \equiv \frac{\sigma^{\rightarrow\uparrow} + \sigma^{\leftarrow\downarrow} - \sigma^{\rightarrow\downarrow} - \sigma^{\leftarrow\uparrow}}{\sigma^{\rightarrow\uparrow}_{int} + \sigma^{\leftarrow\downarrow}_{int} + \sigma^{\rightarrow\downarrow}_{int} + \sigma^{\leftarrow\uparrow}_{int}} = \frac{S_{aL}\, |\vec{S}_{bT}|}{2\pi}\left[A_{LT}^{\cos(\phi-\phi_{S_b})} \cos(\phi - \phi_{S_b}) + D\begin{pmatrix} A_{LT}^{\cos(3\phi-\phi_{S_b})} \cos(3\phi - \phi_{S_b}) \\ + A_{LT}^{\cos(\phi+\phi_{S_b})} \cos(\phi + \phi_{S_b}) \end{pmatrix}\right]$$

$$A_{TT} \equiv \frac{\sigma^{\uparrow\uparrow} + \sigma^{\downarrow\downarrow} - \sigma^{\uparrow\downarrow} - \sigma^{\downarrow\uparrow}}{\sigma^{\uparrow\uparrow}_{int} + \sigma^{\downarrow\downarrow}_{int} + \sigma^{\uparrow\downarrow}_{int} + \sigma^{\downarrow\uparrow}_{int}} = \frac{|\vec{S}_{aT}||\vec{S}_{bT}|}{2\pi}\Big[A_{TT}^{\cos(2\phi-\phi_{S_a}-\phi_{S_b})} \cos(2\phi - \phi_{S_a} - \phi_{S_b}) + A_{TT}^{\cos(\phi_{S_b}-\phi_{S_a})} \cos(\phi_{S_b} - \phi_{S_a})$$
$$+D\Big(A_{TT}^{\cos(\phi_{S_b}+\phi_{S_a})} \cos(\phi_{S_a} + \phi_{S_b}) + A_{TT}^{\cos(4\phi-\phi_{S_a}-\phi_{S_b})} \cos(4\phi - \phi_{S_a} - \phi_{S_b})$$
$$+ A_{TT}^{\cos(2\phi-\phi_{S_a}+\phi_{S_b})} \cos(2\phi - \phi_{S_a} + \phi_{S_b}) + A_{TT}^{\cos(2\phi+\phi_{S_a}-\phi_{S_b})} \cos(2\phi + \phi_{S_a} - \phi_{S_b}) \Big)\Big]$$

The azimuthal asymmetries can be calculated as ratios of cross sections differences to the sum of the integrated over *Φ* cross sections.

The azimuthal distribution of MMT-DY pair's produced in non-polarized hadron collisions, A_{UU}, and azimuthal asymmetries of the cross sections in polarized hadron collisions, A_{jk}, are given by relations shown left.

Physics motivations.

Nucleon spin structure studies using the MMT-DY reactions.
The PDFs studies via asymmetry of the MMT-DY pairs.

Applying the Fourier analysis to the measured asymmetries, one can separate each of all ratios entering previous slide.

This will be the one of task of the experiments proposed for SPD.

The extraction of different TMD PDFs from those ratios is a task of the global theoretical analysis (a challenge for the theoretical community) since each of the SFs a result of convolutions of different TMD PDFs in the quark transverse momentum space.
For this purpose one needs either to assume a factorization of the transverse momentum dependence for each TMD PDFs, having definite mathematic form (usually Gaussian) with some parameters to be fitted (M. Anselmino et al., arXiv:1304.7691 [hep-ph]),
or to transfer to impact parameter representation space and to use the
Bessel weighted TMD PDFs
(Daniel Boer, Leonard Gamberg, Bernhard Musch, Alexei Prokudin, JHEP 1110 (2011) 021, [arXiv:1107.5294])

Physics motivations.

Nucleon spin structure studies using the MMT-DY reactions.
Studies of PDFs via integrated asymmetries.

The set of asymmetries mentioned above gives the access to all eight leading twist TMD PDFs. However, sometimes one can work with integrated asymmetries. Integrated asymmetries are useful for the express analysis of data and checks of expected relations between asymmetries mentioned above. They are also useful for model estimations and determination of required statistics . Let us consider several examples starting from the case when only one of colliding hadrons (for instance, hadron "b") is transversely polarized. In this case the MMT-DY cross section can be reduced to the expression:

$$
\begin{aligned}
\frac{d\sigma}{dx_a dx_b d^2\mathbf{q}_T d\Omega} = \frac{\alpha^2}{4Q^2} \Bigg\{ & (1+\cos^2\theta)\, C\left[f_1 \bar{f}_1 \right] \\
& + \sin^2\theta \cos 2\phi\, C\left[\frac{2(\vec{h}\cdot\vec{k}_{aT})(\vec{h}\cdot\vec{k}_{bT}) - \vec{k}_{aT}\cdot\vec{k}_{bT}}{M_a M_b} h_1^{\perp} \bar{h}_1^{\perp} \right] \\
& + |S_{bT}| \Bigg[(1+\cos^2\theta)\sin(\phi-\phi_{S_b})\, C\left[\frac{\vec{h}\cdot\vec{k}_{bT}}{M_b} f_1 \bar{f}_{1T}^{\perp} \right] - \sin^2\theta \sin(\phi+\phi_{S_b})\, C\left[\frac{\vec{h}\cdot\vec{k}_{aT}}{M_a} h_1^{\perp} \bar{h}_1 \right] \\
& - \sin^2\theta \sin(3\phi-\phi_{S_b})\, C\left[\frac{2(\vec{h}\cdot\vec{k}_{bT})[2(\vec{h}\cdot\vec{k}_{aT})(\vec{h}\cdot\vec{k}_{bT}) - \vec{k}_{aT}\cdot\vec{k}_{bT}] - \vec{k}_{bT}^2(\vec{h}\cdot\vec{k}_{aT})}{2M_a M_b^2} h_1^{\perp} \bar{h}_{1T}^{\perp} \right] \Bigg] \Bigg\}
\end{aligned}
$$

Physics motivations.

Nucleon spin structure studies using the MMT-DY reactions. Studies of PDFs via integrated asymmetries.

$$A_{UT}^{w[\sin(\phi+\phi_S)]}=\frac{\int d\Omega\, d\phi_S \sin(\phi+\phi_S)\left[d\sigma^{\uparrow}-d\sigma^{\downarrow}\right]}{\int d\Omega d\phi_S\left[d\sigma^{\uparrow}+d\sigma^{\downarrow}\right]/2}=-\frac{1}{2}\frac{C\left[\frac{\vec{h}\cdot\vec{k}_{aT}}{M_a}h_1^{\perp}\bar{h}_1\right]}{C\left[f_1\bar{f}_1\right]},$$

$$A_{UT}^{w[\sin(\phi-\phi_S)]}=\frac{\int d\Omega\, d\phi_S \sin(\phi-\phi_S)\left[d\sigma^{\uparrow}-d\sigma^{\downarrow}\right]}{\int d\Omega d\phi_S\left[d\sigma^{\uparrow}+d\sigma^{\downarrow}\right]/2}=\frac{1}{2}\frac{C\left[\frac{\vec{h}\cdot\vec{k}_{bT}}{M_b}f_1\bar{f}_{1T}^{\perp}\right]}{C\left[f_1\bar{f}_1\right]},$$

$$A_{UT}^{w[\sin(3\phi-\phi_S)]}=\frac{\int d\Omega\, d\phi_S \sin(3\phi-\phi_S)\left[d\sigma^{\uparrow}-d\sigma^{\downarrow}\right]}{\int d\Omega d\phi_S\left[d\sigma^{\uparrow}+d\sigma^{\downarrow}\right]/2}=$$

$$=-\frac{1}{2}\frac{C\left[\frac{2(\vec{h}\cdot\vec{k}_{bT})[2(\vec{h}\cdot\vec{k}_{aT})(\vec{h}\cdot\vec{k}_{bT})-\vec{k}_{aT}\cdot\vec{k}_{bT}]-\vec{k}_{bT}^2(\vec{h}\cdot\vec{k}_{aT})}{2M_aM_b^2}h_1^{\perp}\bar{h}_{1T}^{\perp}\right]}{C\left[f_1\bar{f}_1\right]}$$

$$A_{UT}^{w\left[\sin(\phi+\phi_S)\frac{q_T}{M_N}\right]}=\frac{\int d\Omega\int d^2\mathbf{q}_T(|\mathbf{q}_T|/M_p)\sin(\phi+\phi_S)\left[d\sigma^{\uparrow}-d\sigma^{\downarrow}\right]}{\int d\Omega\int d^2\mathbf{q}_T\left[d\sigma^{\uparrow}+d\sigma^{\downarrow}\right]/2}$$

$$=-\frac{\sum_q e_q^2\left[\bar{h}_{1q}^{\perp(1)}(x_p)h_{1q}(x_{p\uparrow})+(q\leftrightarrow\bar{q})\right]}{\sum_q e_q^2\left[\bar{f}_{1q}(x_p)f_{1q}(x_{p\uparrow})+(q\leftrightarrow\bar{q})\right]},$$

$$A_{UT}^{w\left[\sin(\phi-\phi_S)\frac{q_T}{M_N}\right]}=\frac{\int d\Omega\int d^2\mathbf{q}_T(|\mathbf{q}_T|/M_p)\sin(\phi-\phi_S)\left[d\sigma^{\uparrow}-d\sigma^{\downarrow}\right]}{\int d\Omega\int d^2\mathbf{q}_T\left[d\sigma^{\uparrow}+d\sigma^{\downarrow}\right]/2}$$

$$=2\frac{\sum_q e_q^2\left[f_{1T}^{\perp(1)q}(x_{p\uparrow})\bar{f}_{1q}(x_p)+(q\leftrightarrow\bar{q})\right]}{\sum_q e_q^2\left[\bar{f}_{1q}(x_{p\uparrow})f_{1q}(x_p)+(q\leftrightarrow\bar{q})\right]},$$

where

$$h_{1q}^{\perp(1)}(x)=\int d^2k_T\left(\frac{k_T^2}{2M_p^2}\right)h_{1q}^{\perp}(x_p,k_T^2)\quad\text{and}\quad f_{qIT}^{\perp(1)}(x)=\int d^2k_T\left(\frac{k_T^2}{2M_p^2}\right)f_{qIT}^{\perp(1)}(x,k_T^2)$$

The integrated and additionally q_T -weighted asymmetries $A_{UT}^{w\left[\sin(\phi+\phi_S)\frac{q_T}{M_N}\right]}$ and $A_{UT}^{w\left[\sin(\phi-\phi_S)\frac{q_T}{M_N}\right]}$ provide access to the first moments of the Boer-Mulders, $h_{1q}^{\perp}(x,k_T^2)$ and Sivers, $f_{qIT}^{\perp(1)}(x,k_T^2)$

$$A_{UT}^{w\left[\sin(\phi-\phi_S)\frac{q_T}{M_N}\right]}\Bigg|_{x_p>>x_{p\uparrow}}\approx 2\frac{\bar{f}_{1uT}^{\perp(1)}(x_{p\uparrow})}{\bar{f}_{1u}(x_{p\uparrow})}\quad;\quad A_{UT}^{w\left[\sin(\phi+\phi_S)\frac{q_T}{M_N}\right]}\Bigg|_{x_p>>x_{p\uparrow}}\approx-\frac{h_{1u}^{\perp(1)}(x_p)\bar{h}_{1u}(x_{p\uparrow})}{f_{1u}(x_p)\bar{f}_{1u}(x_{p\uparrow})}$$

$$A_{UT}^{w\left[\sin(\phi-\phi_S)\frac{q_T}{M_N}\right]}\Bigg|_{x_p<<x_{p\uparrow}}\approx 2\frac{f_{1uT}^{\perp(1)}(x_{p\uparrow})}{f_{1u}^{\perp(1)}(x_{p\uparrow})}\quad;\quad A_{UT}^{w\left[\sin(\phi+\phi_S)\frac{q_T}{M_N}\right]}\Bigg|_{x_p<<x_{p\uparrow}}\approx-\frac{\bar{h}_{1u}^{\perp(1)}(x_p)h_{1u}(x_{p\uparrow})}{\bar{f}_{1u}(x_p)f_{1u}(x_{p\uparrow})}.$$

A. Sissakian, O. Shevchenko, A. Nagaytsev, and O. Ivanov, arXiv:0807.2480 [hep-ph].
A. Sissakian, O. Shevchenko, A. Nagaytsev and O. Ivanov, Phys. Rev. D72(2005) 054027), [arXiv:hep-ph/0505214].
A. Sissakian, et al., Eur. Phys. J. C46 (2006)147, [arXiv:hep-ph/0512095].

Physics motivations.

Nucleon spin structure studies using the Drell-Yan reactions. Studies of PDFs via integrated asymmetries.

So far the pp-collisions have been considered. At NICA the pd- and dd-collisions will be investigated as well. As it is known from COMPASS experiment, the SIDIS asymmetries on polarized deuterons are consisted with zero. At NICA one can expect that asymmetries

$$A_{UT}^{w\left[\sin(\phi\pm\phi_S)\frac{q_T}{M_N}\right]}\Bigg|_{pD^\uparrow}, \quad A_{UT}^{w\left[\sin(\phi\pm\phi_S)\frac{q_T}{M_N}\right]}\Bigg|_{DD^\uparrow}$$

also will be consistent with zero (subject of tests).

But asymmetries in $Dp\uparrow$ collisions are expected to be non-zero. In the limiting cases $x_D >> x_{p^\uparrow}$ and $x_D << x_{p^\uparrow}$ these asymmetries (**accessible only at NICA**)

$$A_{UT}^{w\left[\sin(\phi-\phi_S)\frac{q_T}{M_N}\right]}(x_D >> x_{p\uparrow})\Bigg|_{Dp\uparrow\to l^+l^-X} \approx \frac{4\,\bar{f}_{1uT}^{\perp(1)}(x_{p\uparrow}) + \bar{f}_{1dT}^{\perp(1)}(x_{p\uparrow})}{4\,\bar{f}_{1u}^{\perp(1)}(x_{p\uparrow}) + \bar{f}_{1d}^{\perp(1)}(x_{p\uparrow})},$$

$$A_{UT}^{w\left[\sin(\phi-\phi_S)\frac{q_T}{M_N}\right]}(x_D << x_{p\uparrow})\Bigg|_{Dp\uparrow\to l^+l^-X} \approx 2\frac{4\,f_{1uT}^{\perp(1)}(x_{p\uparrow}) + f_{1dT}^{\perp(1)}(x_{p\uparrow})}{4\,f_{1u}^{\perp(1)}(x_{p\uparrow}) + f_{1d}^{\perp(1)}(x_{p\uparrow})}.$$

$$A_{TT}^{w[\cos(\phi_{Sb}+\phi_{Sa})q_T/M]} \equiv A_{TT}^{int} = \frac{\sum_q e_q^2\left(\bar{h}_{1q}(x_1)h_{1q}(x_2) + (x_1 \leftrightarrow x_2)\right)}{\sum_q e_q^2\left(\bar{f}_{1q}(x_1)\,f_{1q}(x_2) + (x_1 \leftrightarrow x_2)\right)}.$$

$$A_{UT}^{w\left[\sin(\phi+\phi_S)\frac{q_T}{M_N}\right]}(x_D >> x_{p\uparrow})\Bigg|_{Dp\uparrow\to l^+l^-X} \approx -\frac{[h_{1u}^{\perp(1)}(x_D) + h_{1d}^{\perp(1)}(x_D)][4\bar{h}_{1u}(x_{p\uparrow}) + \bar{h}_{1d}(x_{p\uparrow})]}{[\,f_{1u}(x_D) + f_{1d}(x_D)][4\,\bar{f}_{1u}(x_{p\uparrow}) + \bar{f}_{1d}(x_{p\uparrow})]},$$

$$A_{UT}^{w\left[\sin(\phi+\phi_S)\frac{q_T}{M_N}\right]}(x_D << x_{p\uparrow})\Bigg|_{Dp\uparrow\to l^+l^-X} \approx -\frac{[\bar{h}_{1u}^{\perp(1)}(x_D) + \bar{h}_{1d}^{\perp(1)}(x_D)][4h_{1u}(x_{p\uparrow}) + h_{1d}(x_{p\uparrow})]}{[\,\bar{f}_{1u}(x_D) + \bar{f}_{1d}(x_D)][4\,f_{1u}(x_{p\uparrow}) + f_{1d}(x_{p\uparrow})]}.$$

Proposed measurements.

Estimations of MMT-DY pairs rates.

Estimation of the MMT-DY pair's production rate at SPD was performed using the expression for the differential and total cross sections of the pp interactions:

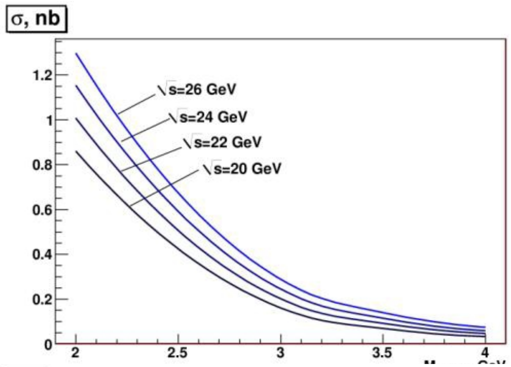

$$\frac{d^2\sigma}{dQ^2dx_1} = \frac{1}{sx_1}\frac{4\pi\alpha^2}{9Q^2}\sum_{f,\bar{f}} e_f^2[f(x_1,Q^2)\bar{f}(x_2,Q^2)]_{x_2=Q^2/sx_1}$$

$$\sigma_{tot} = \int_{Q^2_{min}}^{Q^2_{max}} dQ^2 \int_{x_{min}}^{1} dx_1 \frac{d^2\sigma}{dQ^2dx_1},$$

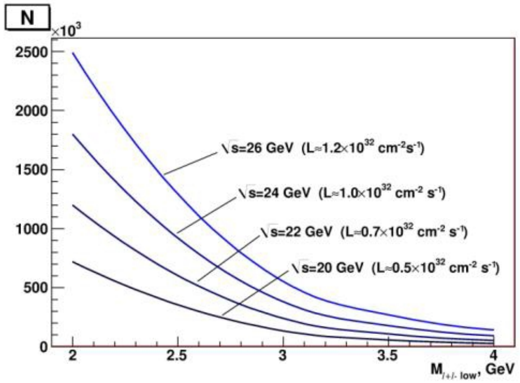

Cross section (left) and number of MMT-DY events (right) versus the minimal invariant mass of lepton pair for various proton beam energies

The Table shows values of the cross sections and expected statistics for MMT-DY events (K events) per four moths of data taking and 100% acceptance of SPD at two energies.

Lower cut on M_{l+l-}, GeV	2.0	3.0	3.5	4.0
$\sqrt{s}$=24 GeV (L = $1.0\cdot10^{32}$ cm^{-2} s^{-1})				
σ_{DY} total, nb	1.15	0.20	0.12	0.06
events	1800	313	179	92
$\sqrt{s}$=26 GeV (L = $1.2\cdot10^{32}$ cm^{-2} s^{-1})				
σ_{DY} total, nb	1.30	0.24	0.14	0.07
events	2490	460	269	142

Proposed measurements.

Estimations of MMT-DY pairs rates.

Statistics of the J/Ψ and MMT-DY events (with cut on $M_{l^-l^+}= 4$ GeV) expected to be recorded ("per year") in four months of data taking with 100% efficiency of SPD are given in Table.

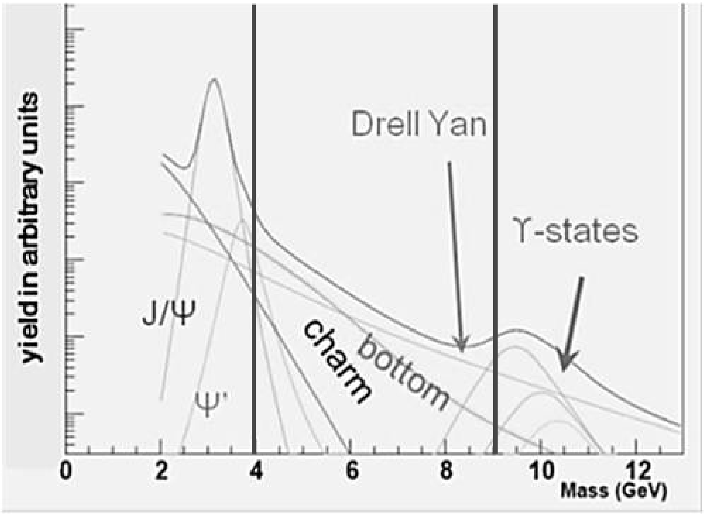

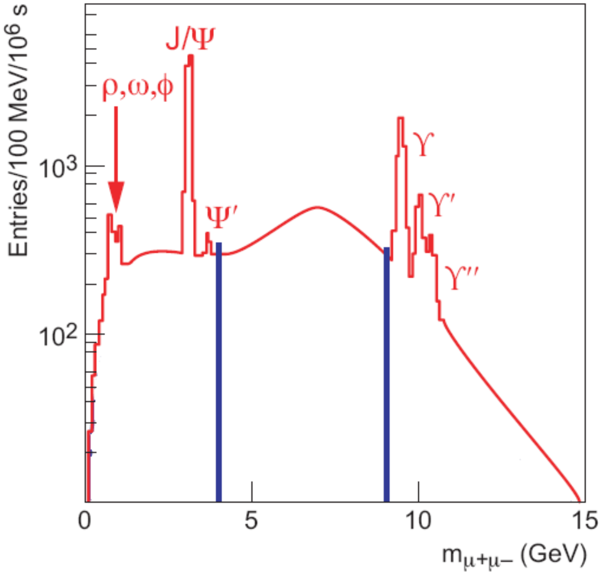

$\sqrt{s}$, GeV	24	26	$\sqrt{s}$, GeV	24	26
$\sigma_{J/\psi} \cdot B_{e+e-}$, nb	12	16	σ_{DY} , nb	0.06	0.07
Events "per year"	$18 \cdot 10^6$	$23 \cdot 10^6$	Events "per year"	$92 \cdot 10^3$	$142 \cdot 10^3$

Proposed measurements.

Estimations of MMT-DY pairs and J/Ψ production rates.

To estimate the precision of measurements, the set of original software packages for MC simulations, including generators for Sivers, Boer-Mulders and Transversity PDFs, were developed in A.Sissakian,O.Shevchenko,A.Nagaytsev,O.Ivanov, Phys.Part.Nucl.41 (2010) 64-100.
With these packages a sample of 100K MMT-DY events was generated in the region of $Q^2 > 11$ GeV^2 for comparison with expected asymmetries.

Fit I: $xf_{1uT}^{\perp(1)} = -xf_{1dT}^{\perp(1)} = 0.4x(1-x)^5$; Fit II: $xf_{1uT}^{\perp(1)} = -xf_{1dT}^{\perp(1)} = 0.1x^{0.3}(1-x)^5$

Fit III: $xf_{1uT}^{\perp(1)} = -xf_{1dT}^{\perp(1)} = (0.17...0.18)x^{0.66}(1-x)^5$

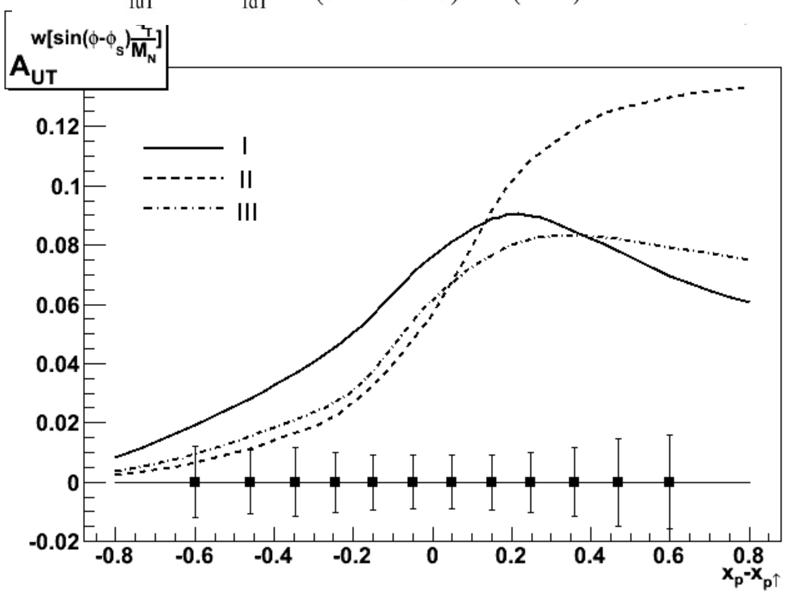

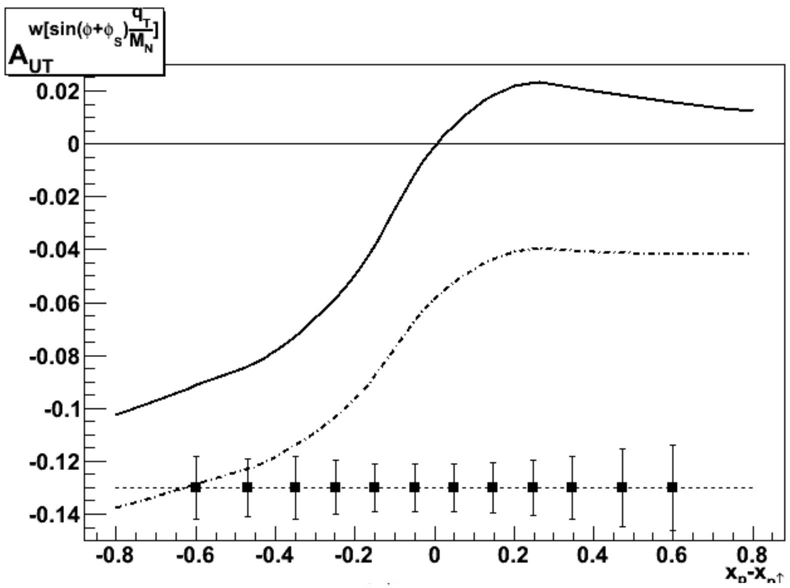

Estimations of Boer-Mulders asymmetry $A_{UT}^{w\left[\sin(\phi+\phi_S)\frac{q_T}{M_N}\right]}$ at $\sqrt{s} = 26$ GeV and $Q^2 = 15$ GeV^2. The solid and dotted curves correspond to the first and second versions of the evolution model, respectively. Points with bars show the expected statistical errors obtained with 100K of events

Estimated Sivers asymmetry $A_{UT}^{w\left[\sin(\phi-\phi_S)\frac{q_T}{M_N}\right]}$ at $\sqrt{s} = 26$ GeV with $Q^2 = 15$ GeV^2.

Proposed measurements.

Extraction of unknown (poor known) parton distribution functions (PDFs):

$$p(D)p(D) \to \gamma^* X \to l^+ l^- X$$

Boer-Mulders PDF

$$p^{\uparrow}(D^{\uparrow})p(D) \to \gamma^* X \to l^+ l^- X$$

Sivers PDFs
(Efremov,… PLB 612 (2005), PRD 73(2006));

$$p^{\uparrow}(D^{\uparrow})p^{\uparrow}(D^{\uparrow}) \to \gamma^* X \to l^+ l^- X$$

Transversity PDF (Anselmino, Efremov, …)

$$p^{\uparrow}(D^{\uparrow})p(D) \to \gamma^* X \to l^+ l^- X$$
$$p(D)p(D) \to \gamma^* X \to l^+ l^- X$$

Transversity and first moment of Boer-Mulders PFDs
(Sissakian, Shevchenko, Nagaytsev , Ivanov, PRD 72(2005), EPJ C46 ,2006 C59, 2009)

$$p^{\rightarrow}(D^{\rightarrow})p^{\leftarrow}(D^{\leftarrow}) \to \gamma^* X \to l^+ l^- X$$

Longitudinally polarized sea and strange PDFs and tenzor deuteron structure
(Teryaev, …)

The same PDFs from J/ψ production processes ($\sqrt{s} \le 10 GeV$).

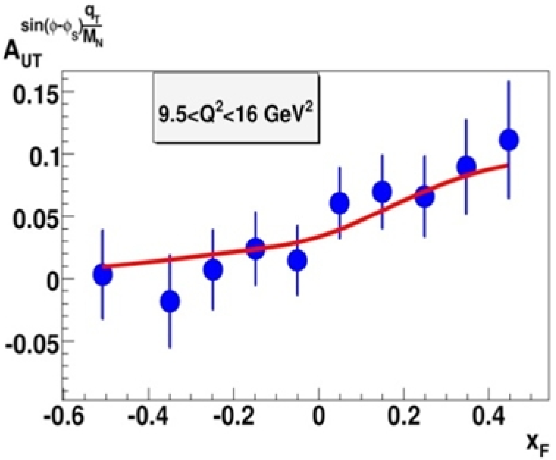

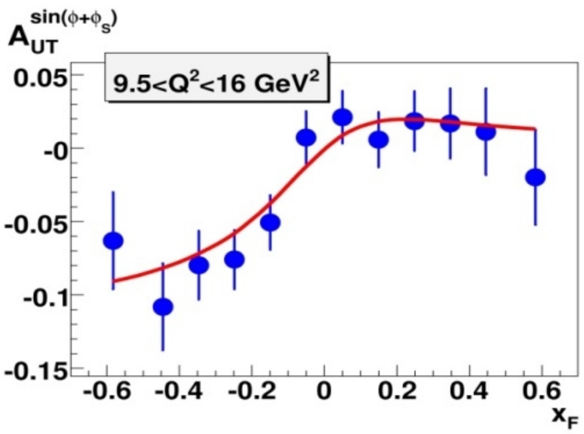

Future DY experiments

The SPD experimentswill have a number of advantages for DY measurements related to nucleon structure studies.
These advantages include:
- operations with pp, pd and dd beams,
- scan of effects on beam energies,
- measurement of effects via muon and electron-positron pairs simultaneously,
- operations with non-polarized, transverse and longitudinally polarized beams or their combinations.
Such possibilities permit for the first time to perform comprehensive studies of all leading twist PDFs of nucleons in a single experiment with minimum systematic errors.

Experiment	CERN, COMPASS-II	FAIR, PANDA	FNAL, E-906	RHIC, STAR	RHIC-PHENIX	NICA, SPD
mode	fixed target	fixed target	fixed target	collider	collider	collider
Beam/target	π- , p	anti-p,p	π- , p	pp	pp	pp, pD,DD
Polarization: beam, target	0; ~ 0.8	0; 0	0; 0;	0.5 ; 0.5	0.5 ; 0.5	0.5 ; 0.5
Luminosity, $cm^{-2}s^{-1}$	10^{32}	10^{32}	10^{42}	10^{32}	10^{32}	10^{32}
$\sqrt{s}$, *GeV*	17	6	16	200	200	10-26
$x_{1(beam)}$ $x_{2(targ)}$ ranges	0.1-1.0 ; 0.5-0.9	0.1-1.0 ; 0.3-0.8	0.1-1.0 ; 0.3-0.8	0.1-0.9 ; 0.1-0.9	0.1-0.9 ; 0.1-0.9	0.1-0.8 ; 0.1-0.8
q_T, GeV	0.5 -4.0	0.5 -1.5	0.5 -3.0	1.0 -10.0	1.0 -10.0	0.5 -6.0
Lepton pairs,	μ-μ+	μ-μ+	μ-μ+	μ-μ+	μ-μ+	μ-μ+, *e+e-*
Data taking	2014	>2018	2013	>2016	>2016	>2017
Transversity PDF	YES	NO	NO	YES	YES	YES
Boer-Mulders PDF	YES, valence, $h_{1(\pi)}^{\perp} \otimes h_{1(p)}^{\perp}$	YES	YES	YES	YES	YES
Sivers PDF	YES, π PDF	YES	YES	YES	YES	YES
Pretzelosity PDF	YES	NO	NO	NO	YES	YES
Worm Gear PDFs	YES	NO	NO	NO	NO	YES
Duality, J/Ψ	YES	YES	NO	NO	NO	YES
Flavour decomposition	NO	NO	YES	NO	NO	YES
Lam-Tung relation	NO	NO	NO	NO	NO	YES

Requirements to SPD

Required characteristics of the experimental setup:

- Geometry close to 4π,
- high-precision (better than 50 μm) and fast vertex detector,
- a tracking system that provides high accuracy (~200 μm) along the track,
- DAQ- data taking rate for luminosity> 10^{32},
- minimum of material,
- measurement of neutral (π^0 etc) secondary particles,
- Identification of charged particles with efficiency close to 100%,
- fast and modern trigger system,
- Modularity and access to the elements of the setup, which will allow to upgrade and modify detectors for new research.

Tracking detectors:

- Vertex detector - several coordinate silicon layers with resolution of the order of 30 μm;
-central and end track detectors - several groups of layers of straw tubes;
-100% effi – to reduce background to MMT-DY
- In addition, you can use the space between the windings of the toroidal a magnet for drift chambers. Track resolution ~ 300 μm.

Trigger detectors:

- signals from the electromagnetic calorimeter ("shashlyk" - as for COMPASS);
- scintillation plates.
It is necessary to organize different types of triggers.

PID detectors:

- Time-of-flight system from - RPC planes;
- electromagnetic calorimeter;
- muon system.

Requirements to SPD.Vertex detector

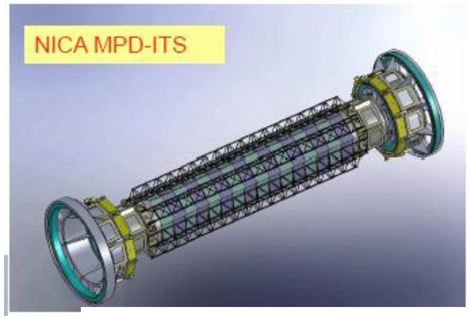

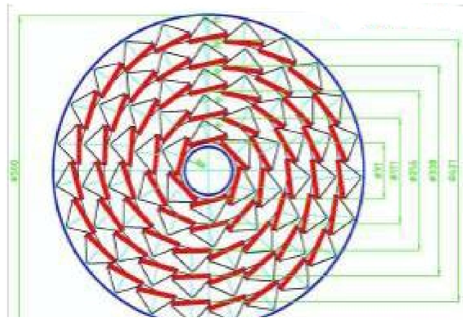

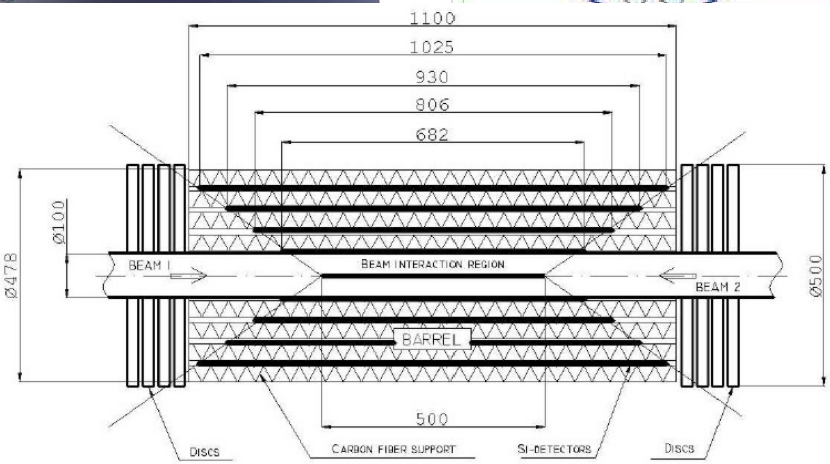

Total number of detectors 806

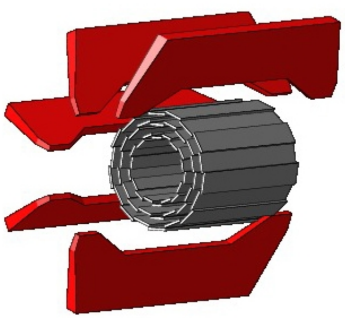

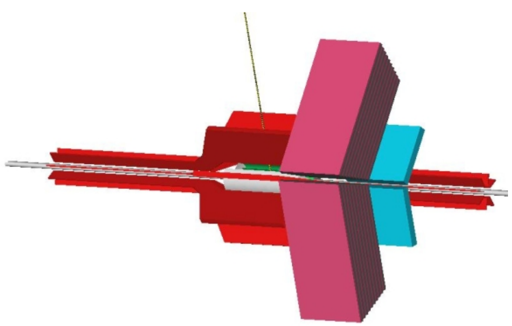

Silicon Microvertex Detector

Outside the beam pipe. Several layers of double sided silicon strips can provide a precise vertex reconstruction and tracking of the particles before they reach the general SPD tracking system. The design should use a small number of silicon layers to minimize the radiation length of the material. With a pitch of 50-100 µm it is possible to reach the spatial resolution of 20-30 µm. Such a spatial resolution would provide 50-80 µm for precision of the vertex reconstruction. This permits to reject the secondary decay vertexes.

Requirements to SPD. Central Tracker

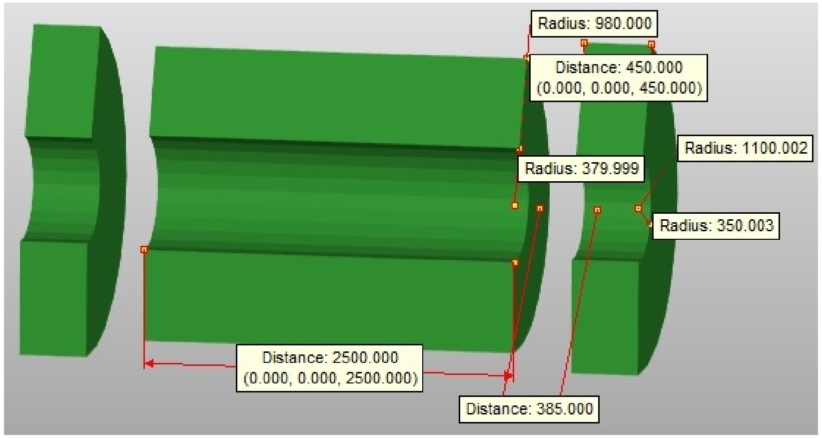

The straw tubes can be selected to be the main detector of SPD Tracking System. This choice is based to the following properties of the staws tubes:

-the minimun of material X_0 ~ 0.1;

- the time resolution ~ 200-300 ns) ;

- spatial track resolution ~ 50-100 µm;

-expected particle rates (DAQ rates ~ 100 Khz);

-Effi ~ 100%;

- production sites in JINR,Dubna.

It is important to stress that the overall physics performance of NA62 depends on a number of experimental necessities for the Straw Tracker:

- Use of ultra-light material along the particle trajectory in order to minimize multiple Coulomb scattering, in particular, near the first chamber.
- Integration of the tracker inside the vacuum tank.
- An intrinsic spatial resolution that allows a precise reconstruction of the intersection point between the decay and parent particle.
- Average track efficiency near 100%.
- Capability to veto events with multiple charged particles
- Sufficient lever arm between the four chambers allowing to re-use the exiting dipole magnet.

From these constrains follow the main requirements of the detector:
- Spatial resolution ≤ 130 µ m per coordinate and ≤ 80 µ m per space point ≤ 0.5% of a radiation length (X 0) for each chamber;
- Installation inside the vacuum tank (P = 10 -5 mbar) with minimum gas load for the vacuum system
- For straws near the beam, operation in a high rate environment (up to 40 kHz/cm, and up to 500 kHz/Straw)
- Contribution as multiplicity veto to the trigger

Requirements to SPD. Central Tracker

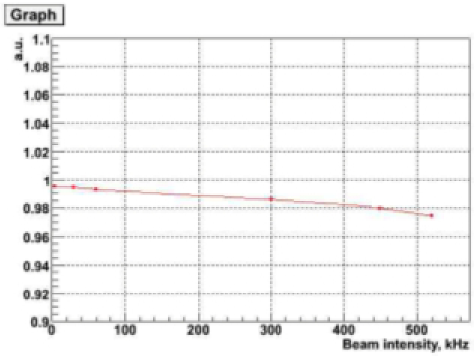

Figure 9. Straw efficiency versus particle rate in a straw.

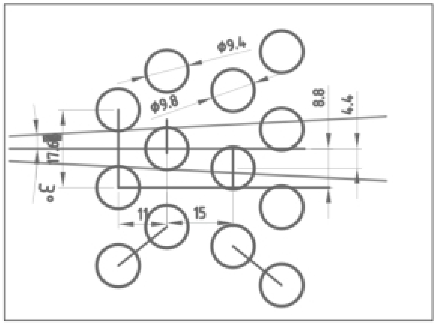

Figure 10. Straw layout in one view (beam direction from left to right). The distance between the straws in one layer is 17.6mm.

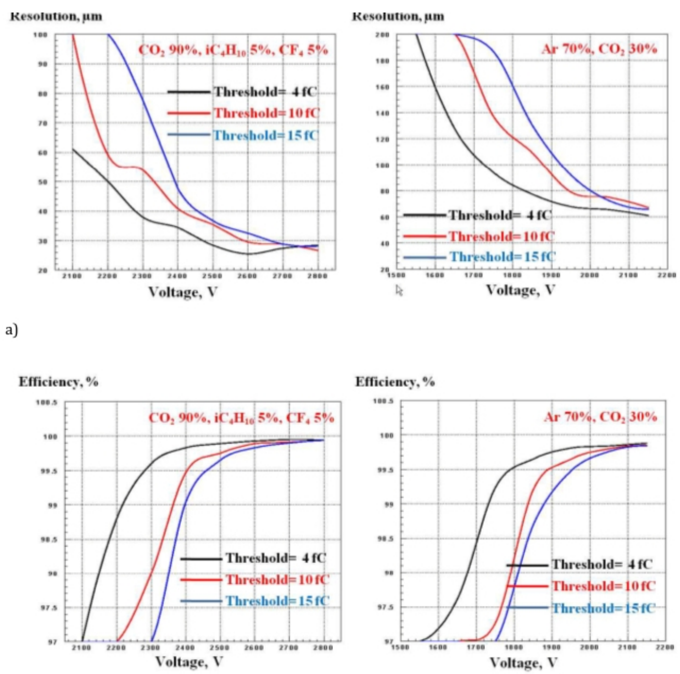

Figure 4. The dependence of the spatial resolution (a) and the straw efficiency (b) on the high voltage and on the threshold for the gas mixtures CO_2 90%, iC_4H_{10} 5%, CF_4 5% and Ar 70%, CO_2 30%. The spatial resolution was calculated for a distance to the straw wire of 3 mm.

NA62 Straw Tracker

Table 1. The main parameters of the straw tracker.

Chamber layout	Value	Comment
Number of chambers	4	
Number of views/chamber	4	
Number of straw layers/view	4	
Number of straws/view	448	
Central gap	~12 cm	
Central gap off-set vs. beam axis	X / Y / U=V	Beam shifted towards the Jura side
Chamber 1	101.2 mm / 0 / 70.4 mm	
Chamber 2	114.4 mm / 0 / 79.2 mm	
Chamber 3	92.4 mm / 0 / 66 mm	
Chamber 4	52.8 mm / 0 / 39.6 mm	
Track angle coverage	± 3°	
Straw length	210	Active length
Straw position accuracy	±0.1mm	
Wire	30 µm gold-plated Tungsten	Toschiba
Straw inner diameter	9.75 ± 0.05 mm	
Straw straightness	±0.1mm	
Maximum wire off-set	0.2 mm	
Gas volume in one straw	160 cm^3	
Straw material (option 1)		
Mylar film	36 µm	Hostaphan RNK 2600
Density	1.39 g/cm^2	
Copper layer	500 Å	
Gold layer	200 Å	
Material budget (1 view)	**Radiation length in %**	
Gas	0.010	
Straw wall	0.099	
Wires	0.0046	
Total	0.1136	
Straw operating conditions		Inner most straws
Wire tension	(90 ± 10) g	
Gas	70% Argon ,30%CO_2	Option: 90%CO_2,5%Isobutan,5%CF_4
High Voltage	1.75 kV	Option: 2.5kV
Gain	1*10^5	
Cathode resistivity	~70 ohm/	
Max Counting rate/straw	0.5 MHz	
High rate per unit area	40 kHz/cm^2	Straws close to center gap
Accumulated charge	0.015 C/cm/year	50 000 bursts of 3s
Maximum current/cm	64 nA/cm	
Gas flow per straw / per view	160 cm^3/h / 70 l/h	High flow straws
Gas pressure (absolute)	1.02-1.04 bar	
Nominal electron drift time	140 ns	
Nominal ion drift time	100 µs	
Effective radius	4.8 mm	>95% efficiency
Cross-talk	3%	Estimated
Nominal threshold	3 fC	5 fC
Termination resistor (far end)	330 Ohm	Estimated

Requirements to SPD. Muon system.

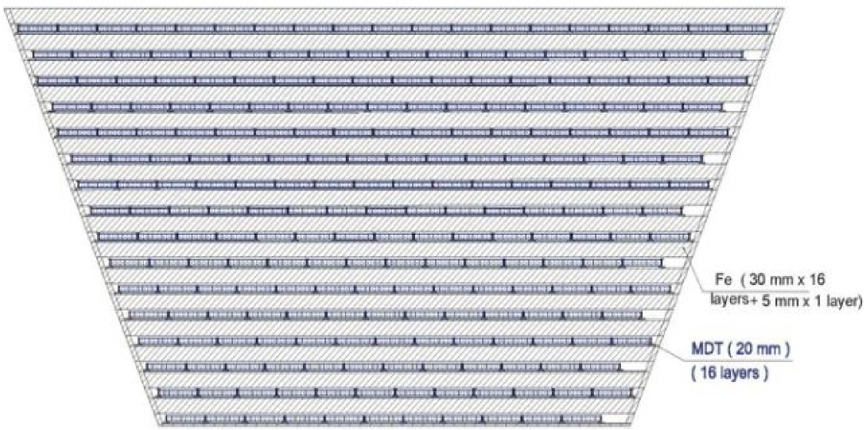

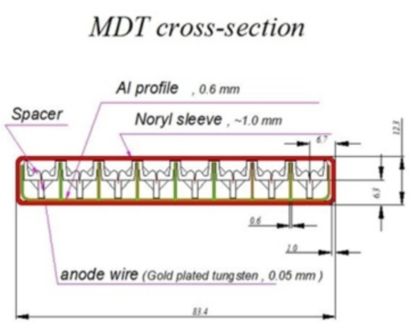

The system of MDT layers with Fe layers called by Range System (RS) is used in SPD as moun detector and main element of Particle Identification System.
It can provide the clean (>95%) muon identification for muon momenta grater than 1 GeV.
The combination of responses from EM calorimeter and RS can be used for the identification of pions and protons in the wide energy range.
RS provides good coordinate accuracy.

Plots are from " Muon TDR for PANDA ", PANDA Collab., November 2011

V.Abazov et al., Instrum.Exp.Tech.53:648-652,2010, Prib.Tekh.Eksp.5:32-36,2010.

DLNP group, leader G.Alexeev

Requirements to SPD. Muon system.

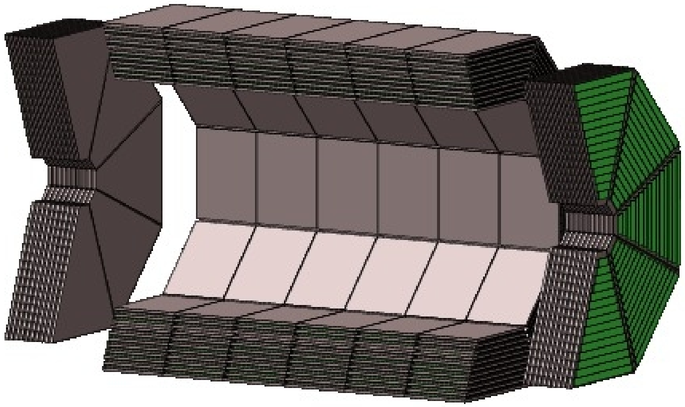

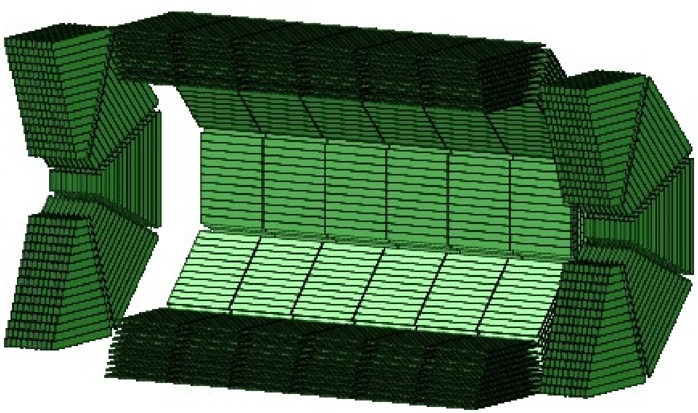

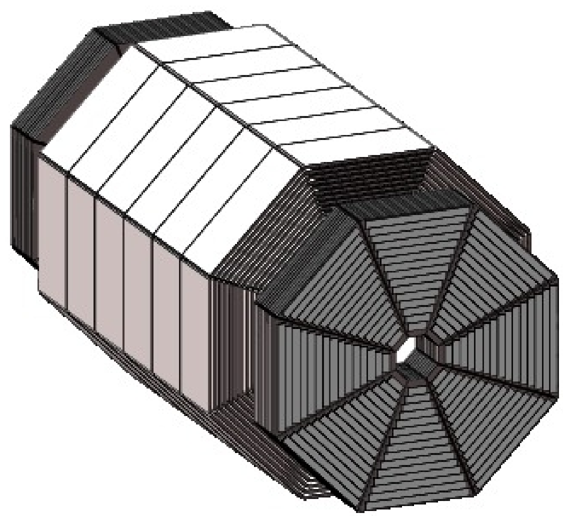

The Range System consists of two parts: Barrel and two End cups.

The preliminary sizes of RS are as follows: about 6.8 m along beam line and 3.7 m in diameter.

The RS designed with consists of 4140 MDT units for barell, 2x1200 units for End-cups.

Total: 6540 ch.

Requirements to SPD. Muon system.

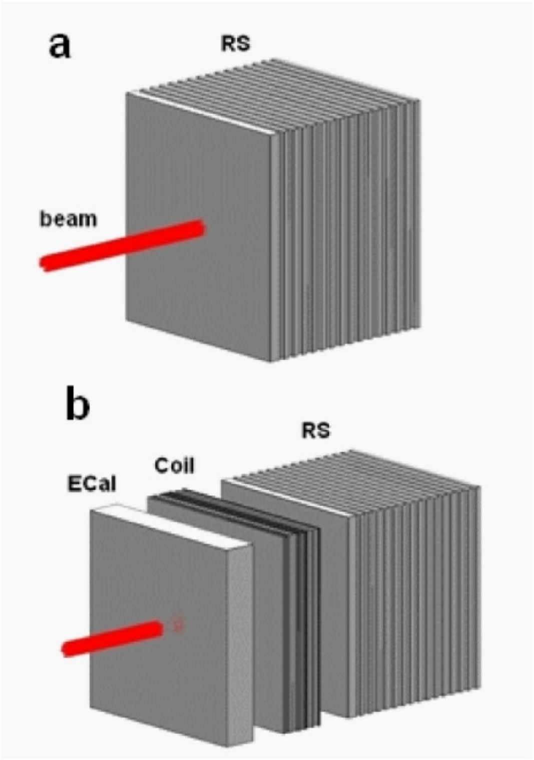

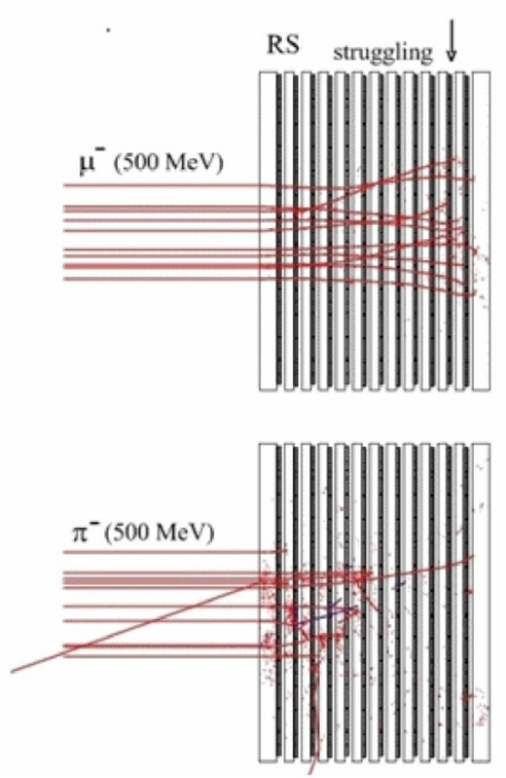

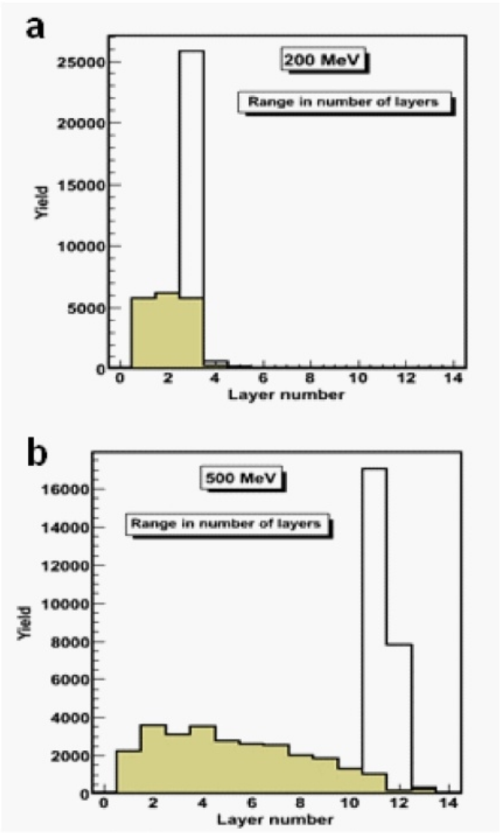

Plots are from " Muon TDR for PANDA ", PANDA Collab., November 2011

Requirements to SPD. Muon system.

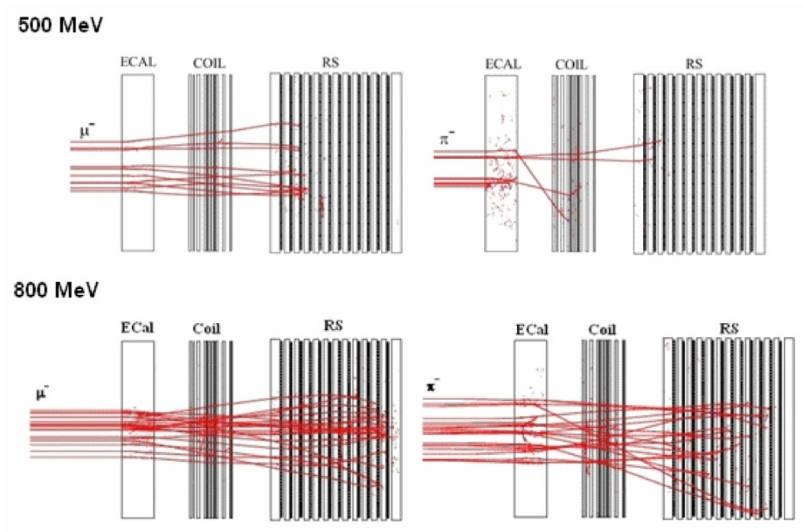

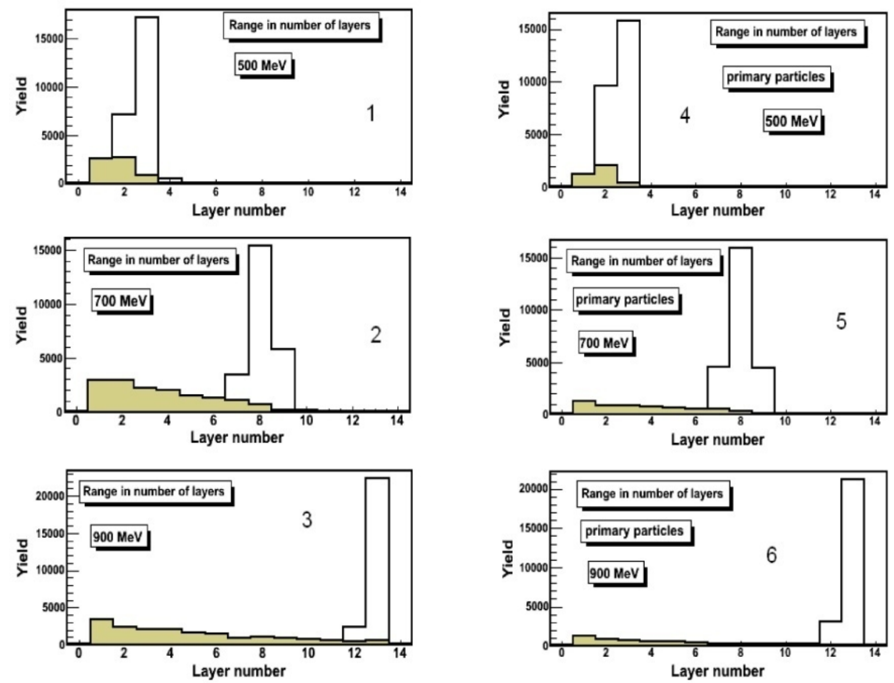

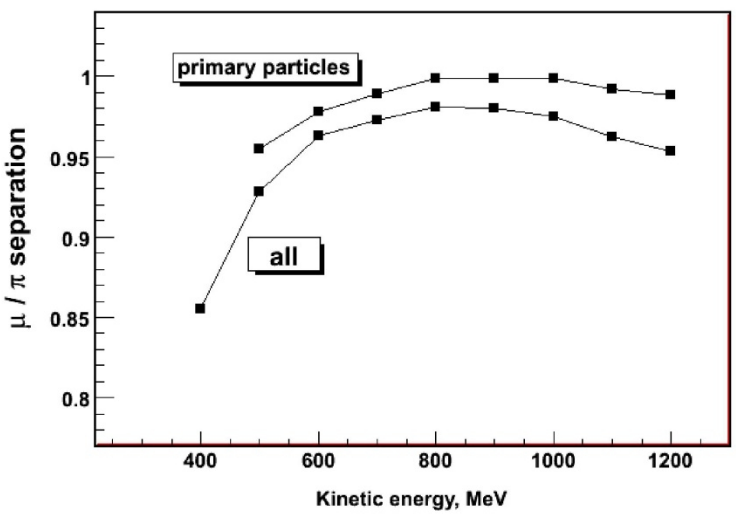

Estimated μ/π for E>1 GeV is more than 96%

Plots are from “ Muon TDR for PANDA ”, PANDA Collab., November 2011

MMT-DY with SPD. Manpower and plans.

1. SPD design.
   - toroid vs solenoid;
   - optimization detector's geometry;
   - absorber ?
2. SPD resolutions and effi for MMT-DY.
3. MC background studied.
4. PDFs and SFs extraction.
5. Statistical projections on asymmetries
5. MMT-DY contribution to CDR.

For next SPD meetings:

- talk on BG studies,
- talk on MMT-DY events with toroidal field

A.Nagaytsev
G.Meshcheryakov
R.Akhunzyanov
A.Ivanov
+ 1-2 members from Tomsk team

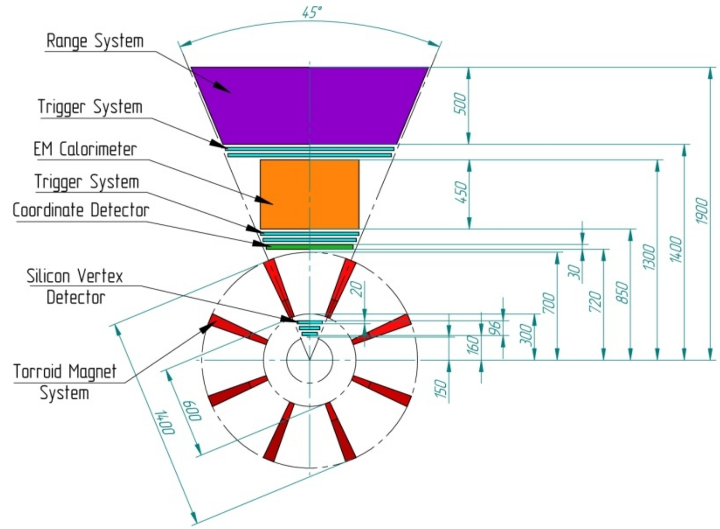

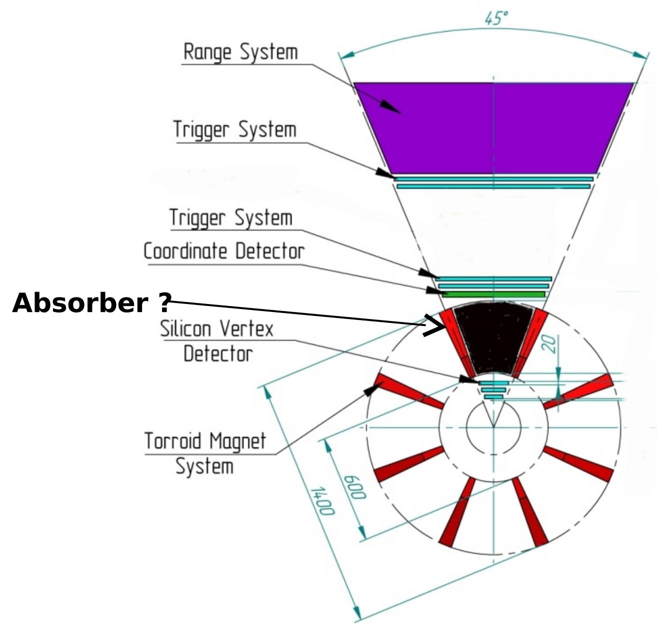

Nec sine te, nec tecum vivere possum. (Ovid)*

MMT-DY with SPD.
Old kinematical plots.